

Supplementary Materials for

Ultra-compact broadband polarization diversity orbital angular momentum generator with $3.6 \times 3.6 \mu\text{m}^2$ footprint

Nan Zhou, Shuang Zheng, Xiaoping Cao, Yifan Zhao, Shengqian Gao, Yuntao Zhu, Mingbo He, Xinlun Cai*, Jian Wang*

*Corresponding author. Email: caixlun5@mail.sysu.edu.cn (X.C.); jwang@hust.edu.cn (J.W.)

Published 31 May 2019, *Sci. Adv.* **5**, eaau9593 (2019)

DOI: 10.1126/sciadv.aau9593

This PDF file includes:

Section S1. Evolution process of in-plane guided mode to out-plane OAM mode

Section S2. Device fabrication process

Section S3. Simulated intensity distribution matrix

Fig. S1. Simulated 3D-FDTD results of electric field distributions (real part of electric field components) along the waveguide (from waveguide region to grating region) and at different height of the fork grating region ($z = 0.1, 0.2, 0.3, 0.4, 0.5 \mu\text{m}$, far field).

Fig. S2. Illustration of the device fabrication process of the silicon OAM generator (spin coating, electron-beam lithography, inductively coupled plasma, photoresist removal).

Fig. S3. Simulated 4×4 intensity distribution matrix for the generation of polarization diversity OAM modes (x-pol. OAM₊₁, x-pol. OAM₋₁, y-pol. OAM₊₁, y-pol. OAM₋₁).

Section S1. Evolution process of in-plane guided mode to out-plane OAM mode

To show the evolution process of in-plane guided mode to out-plane OAM mode in free space, we use the 3D finite-difference time-domain (3D-FDTD) method to simulate the electrical field distributions along the waveguide (from waveguide region to grating region) and at different height of the grating region ($z=0.1, 0.2, 0.3, 0.4, 0.5 \mu\text{m}$, far field). The length l of the grating region is $3.6 \mu\text{m}$, the height of the silicon layer is 220 nm , and the etching depth h is 60 nm . Note that $z=0$ means the bottom of the silicon layer. The simulated real part distributions of the electric field components are depicted in Figs. S1A-S1D, respectively. The corresponding amplitude distributions of the electric field components are in the main text (Figs. 3E-3H).

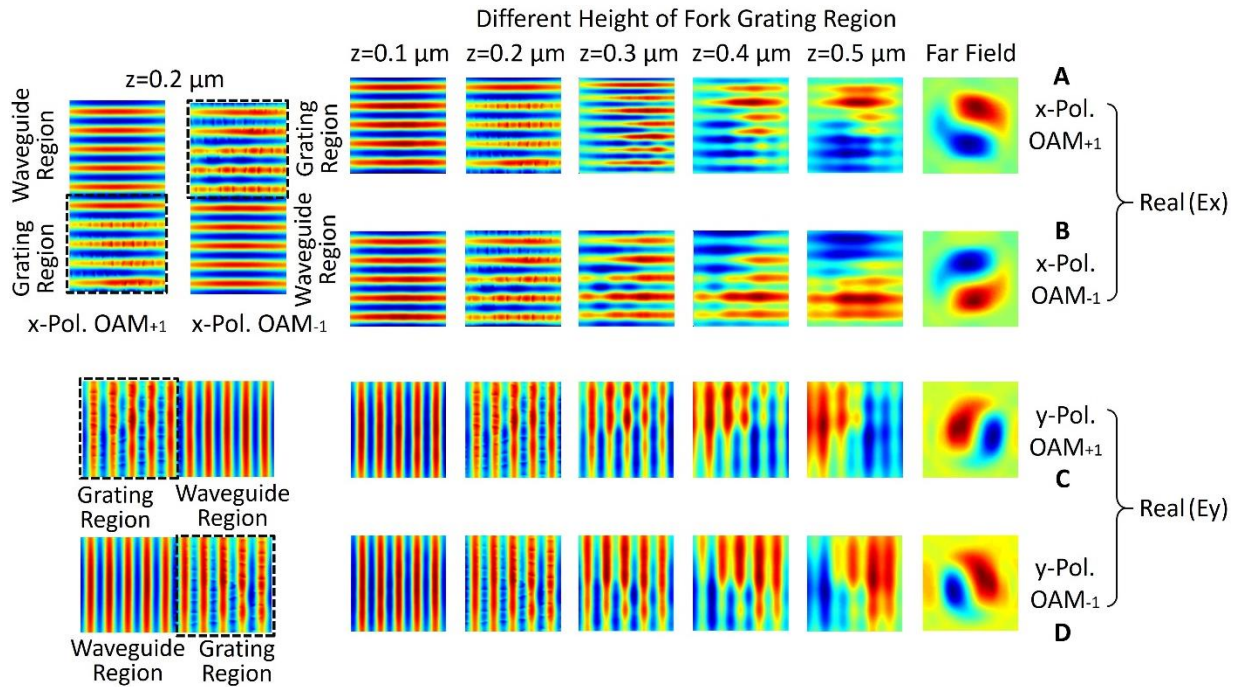


Fig. S1. Simulated 3D-FDTD results of electric field distributions (real part of electric field components) along the waveguide (from waveguide region to grating region) and at different height of the fork grating region ($z = 0.1, 0.2, 0.3, 0.4, 0.5 \mu\text{m}$, far field). (A-D) Polarization diversity OAM generation of x-pol. OAM_{+1} (A), x-pol. OAM_{-1} (B), y-pol. OAM_{+1} (C) and y-pol. OAM_{-1} (D).

As displayed in Figs. S1A-S1D, one can see the mode evolution from the travelling waveguide region to the superposed holographic fork gratings region. Moreover, one can also observe the mode evolution from the in-plane guided mode to out-plane mode in free space by monitoring the electric field distributions (real part) at different height of the grating region. The evolution processes for the generation of all four polarization diversity OAM modes (x-pol. OAM₊₁, x-pol. OAM₋₁, y-pol. OAM₊₁, y-pol. OAM₋₁) under different incident conditions are all shown in Fig. S1.

Section S2. Device fabrication process

As illustrated in Fig. S2, the designed chip-scale broadband polarization diversity OAM generator is fabricated on a standard silicon-on-insulator (SOI) wafer with a 220-nm-thick top silicon layer and a 2- μm -thick buried oxide (SiO₂) layer. In the fabrication process, the layout pattern is defined using the electron-beam lithography (EBL). A positive e-beam resist (ZEP520A) is employed owing to its high dry etch resistance and high resolution. The photonic structure is then transferred to the silicon layer via an inductively coupled plasma (ICP) etching process, followed by resist removal with dimethylacetamide. Waveguides outlines are etched fully down 220 nm to the buried oxide, while gratings are shallow etched down nominally 60 nm. After that, a 1- μm -thick SiO₂ layer is deposited on the top by plasma enhanced chemical vapor deposition (PECVD), covering the whole device as the upper cladding.

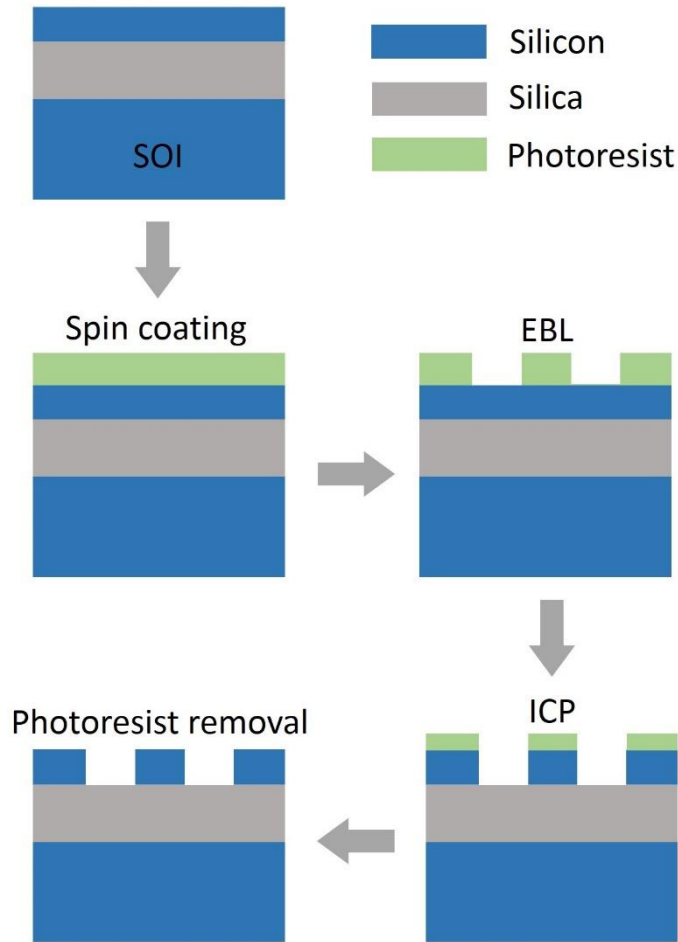


Fig. S2. Illustration of the device fabrication process of the silicon OAM generator (spin coating, electron-beam lithography, inductively coupled plasma, photoresist removal). Shallow and full etching and PECVD upper SiO₂ cladding are not shown here.

Section S3. Simulated intensity distribution matrix

Figure S3 shows the simulated 4x4 intensity distribution matrix for the generation of polarization diversity OAM modes. The diagonal elements in the matrix correspond to the correct detection of both polarization state and OAM state, while the nondiagonal elements are the offset detection. The correct detection of the OAM mode, by loading an inverse phase pattern onto the spatial light modulator (SLM), gives a Gaussian-like beam with bright spot at the beam center.

By comparison, the offset detection of the OAM mode, i.e. the OAM mode is not detected with its corresponding inverse phase pattern, still gives an OAM mode but with an updated charge value and a donut-shaped intensity distribution. The updated OAM mode shows donut-shaped intensity distribution with null intensity at the beam center. Hence, the diagonal elements in the matrix have central bright spots, while the nondiagonal elements in the matrix have null intensity at the center. A piece of fiber can be used for spatial filtering marked as red dashed circles. Assisted by the fiber spatial filtering, the diagonal elements with central bright spots can be coupled into the fiber, while the nondiagonal elements with null intensity at the center will be blocked by the fiber.

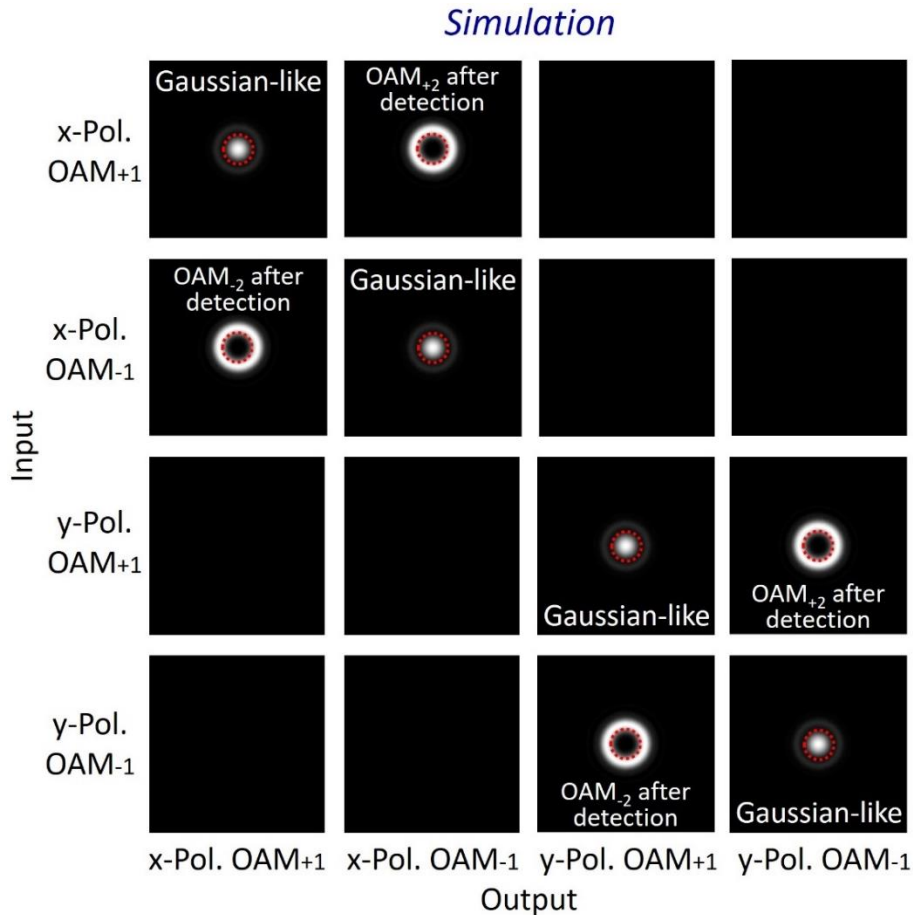


Fig. S3. Simulated 4×4 intensity distribution matrix for the generation of polarization diversity OAM modes (x-pol. OAM₊₁, x-pol. OAM₋₁, y-pol. OAM₊₁, y-pol. OAM₋₁). The red dashed circles mark the spatial filtering region by a piece of fiber.